İSTANBUL UNIVERSITY CERRAHPAŞA

ORIGINAL ARTICLE
Electrica 2022; 22(2): 188-197

The Effects of Operating Frequency on Wireless Power Transfer System Design and Human Health in Electric Vehicles

Ali Ağçal, Tuğba Halime Doğan, Galip Aksu

Department of Electrical and Electronics Engineering, Süleyman Demirel University, Isparta, Turkey

Cite this article as: A. Ağçal, T. H. Doğan and G. Aksu, "The effects of operating frequency on wireless power transfer system design and human health in electric vehicles," *Electrica.*, 22(2), 188-197, 2022.

ABSTRACT

Wireless power transfer (WPT) continues to be popular in today's world because it is used in situations where the use of cables is difficult, dangerous, or restrictive. In WPT, electrical energy is transmitted over the air by magnetic connections instead of cables. In this paper, WPT system designs were made with 10 kHz and 20 kHz operating frequencies, 3.3 kW output power, and 50 cm × 50 cm size. The effects of the frequency on the WPT system were analyzed with the designs made for two separate frequencies. The WPT circuits were established in the MATLAB/Simulink program. The coil design of the WPT systems was made in ANSYS® Maxwell 3D. The critical air gap values of the 10 kHz and 20 kHz designs were determined as 15 cm and 17 cm, respectively. In this study, the efficiency of the WPT system was obtained as 88.79% at 15 cm air gap for 10 kHz and 92.74% at 17 cm air gap for 20 kHz. Wireless power transfer systems in different frequency bands at the same power were compared in terms of efficiency, loss, cost, and electromagnetic field distribution. In addition, the effects of WPT systems on human health were examined according to IEEE and ICNIRP standards.

***Index Terms*—**Human health effects, magnetic resonance coupling, wireless power transfer

I. INTRODUCTION

The wireless power transfer (WPT) has been studied since the 1890s and it has not lost its importance since then. Nicola Tesla has shown that resonance must be used so that energy can be transferred wirelessly efficiently. The transmission of energy via cable has several disadvantages. Cable pollution occurs due to the increasing use of electrical devices. Underwater energy transfers, made through cables, can be dangerous. The simplicity and reliability of the WPT offer a very good solution to avoid these problems. Nowadays, the WPT can be used in electric vehicles [1-3], biomedical devices [4], mobile phones, unmanned aerial vehicles, and many more applications.

The WPT can be done in various ways. These are electromagnetic radiation, microwave, laser, capacitive coupling, inductive coupling, and magnetic resonance coupling methods. The WPT with electromagnetic radiation [5] in the 1900s and microwave [6] in the 1950s were attempted, but due to the low efficiency, it could not become widespread for many years. The widespread use of WPT systems started with the inductive coupling method. Thanks to the inductive coupling method, better efficiency can be obtained in the low-frequency range and short distances compared to other methods [7]. Nowadays, magnetic resonance coupling is the most commonly used theory in WPT systems [8]. This theory was first started by lighting a 60-W lamp from a distance of 2 m without using a cable [9].

Recently, the WPT designs for electric vehicles have taken an important place in the literature [1]. Wireless energy transfer in electric vehicles is developing in many different areas such as different core geometry designs [3], effects on human health [2], and distance extension studies by using additional coil structures [10].

The effect of air gap on efficiency in magnetic resonance coupling circuit was examined by using the Neumann formula. Optimum characteristic impedances were calculated for different air gaps, and according to these values, it was explained by the equations that the system had a high-efficiency double or single resonance frequency [11]. The effects of load impedance on resonance frequency bifurcation and determination of optimum load impedance have been studied [12].

Corresponding author:
Ali Ağçal

E-mail: aliagcal@sdu.edu.tr

Received: February 17, 2022

Accepted: February 28, 2022.

DOI: 10.54614/electrica.2022.22020

In order to keep the efficiency high at the resonant frequency, the effect of the series capacitance value on the input impedance was analyzed [13]. In another study to increase the efficiency of the WPT system, the optimal duty cycle was determined by changing the inverter duty cycle [14].

In this study, WPT system designs operating in two different frequency bands with the same power and dimensions for wireless charging of electric vehicles were made, and the effects of frequency on the WPT system were examined by comparing the two designs. The designed WPT system has 3.3 kW output power, 50 cm × 50 cm size, and 10 kHz and 20 kHz operating frequency. The WPT system is designed with Series-Series (SS) circuit topology using the magnetic resonance coupling method. The effects of frequency on efficiency, air gap, coil design, and internal resistance were analyzed for WPT systems with two different frequencies. In addition, the mutual inductance variation was observed according to different air gaps of both 10 kHz and 20 kHz WPT systems. In the WPT circuit, the inductance values of the receiver and transmitter coil and the capacitance values were obtained by analytical equations. Analytical solution of the circuits was done in MATLAB program, and Finite Element Method (FEM)-based co-simulation was made in ANSYS® Simplorer program. The coil design of the WPT systems was made using the ANSYS® Maxwell 3D program. The effects of the WPT design on human health were analyzed according to IEEE and ICNIRP standards using the ANSYS High Frequency Simulation Software (HFSS) program.

II. MAGNETIC RESONANCE COUPLING

In electrical circuits, an energy oscillation occurs between a capacitor and an inductance connected to each other at a resonant frequency. In the WPT system using magnetic resonance coupling theory, the energy flow from the transmitter to the receiver is maximum at the resonant frequency. The magnetic resonance coupling circuit using SS topology is shown in Fig. 1.

In the equivalent circuit, I_1 and I_2 stand for input current (transmitter current) and output current (receiver current). V_1 is the sinusoidal voltage source of the transmitter circuit. R_1 and R_2 represent transmitter and receiver inner resistance, respectively. R_L is the load resistance. L_1, L_2, and L_m are transmitter inductance, receiver inductance, and mutual inductance, respectively. C_1 and C_2 show the transmitter and receiver resonant capacitors, respectively. The natural angular resonance frequency of the resonator is given in (1) and the quality factor is given in (2):

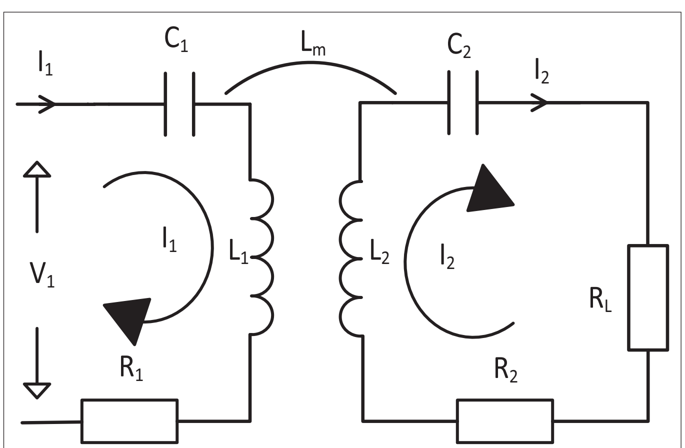

Fig. 1. Magnetic resonance coupling circuit using series-series topology.

$$\omega_0 = \frac{1}{\sqrt{LC}} \tag{1}$$

$$Q = \sqrt{\frac{L}{C}} \times \frac{1}{R} = \frac{\omega_o L}{R} \tag{2}$$

The relationship between the coupling factor (k) and the mutual inductance is given in (3):

$$L_m = k\sqrt{L_1 L_2} \tag{3}$$

The equivalent impedance is given in (6). The efficiency was obtained as in (7) [15]:

$$Z_1 = R_1 + j\omega L_1 \tag{4}$$

$$Z_2 = R_2 + j\omega L_2 \tag{5}$$

$$Z_{Eq} = Z_1 + \left(\frac{1}{j\omega C_1}\right) + \left(\frac{L_m^2\omega^2}{Z_2 + \frac{1}{j\omega C_2} + R_L}\right) \tag{6}$$

$$\eta = \left(\frac{jL_m\omega}{Z_2 + \left(\frac{1}{j\omega C_2}\right) + R_L}\right)^2 \times \frac{R_L}{Z_{Eq}} \tag{7}$$

Z_{Eq} is the equivalent impedance, ω is the angular velocity, and η is the efficiency. Critical mutual inductance is the minimum mutual inductance value at which the WPT system can operate with maximum efficiency and its value is calculated by (8). If the mutual inductance is below the critical mutual inductance as in (9), the efficiency of the WPT system is below the maximum efficiency and the efficiency drops drastically as the mutual inductance decreases. As in (10), if the mutual inductance is above the critical mutual inductance, the WPT system is in the maximum efficient operating region, but bifurcation occurs at the resonance frequencies:

$$L_{m_{critical}}^2 = \frac{Z_0^2 - R^2}{\omega^2} \tag{8}$$

$$L_m^2 < \frac{Z_0^2 - R^2}{\omega^2} \tag{9}$$

$$L_m^2 > \frac{Z_0^2 - R^2}{\omega^2} \tag{10}$$

III. WIRELESS POWER TRANSFER SYSTEM DESIGN

In this WPT design, the operating frequencies were determined as 10 and 20 kHz, and the working size was determined as 50 cm × 50 cm.

The analytical solution of the WPT circuit is made in the MATLAB program. The quality factor (Q) is approximately 100, the internal resistance of a coil is 0.206 Ω for 10 kHz and 0.14 Ω for 20 kHz. Equation (11) gives the self-inductance value according to the quality factor of the resonator, natural resonance frequency, and internal resistance by (2):

$$L = Q \times \frac{R}{2\pi f} \tag{11}$$

The inductance value was found to be $L_{10kHz} = 397$ μH for 10 kHz and $L_{20kHz} = 198.94$ μH for 20 kHz from (11). Capacitor value depending on the inductance value and the angular frequency was obtained as per (12) by using (1):

$$C = \frac{1}{L} \times \omega^2 \tag{12}$$

The resonance capacitors are $C_{10kHz} = 636$ nF for 10 kHz and $C_{20kHz} = 319.85$ nF for 20 kHz. The load resistance is taken as 5 Ω. Calculations were made by creating two different statuses for the coupling coefficient 0.1 and 0.5. The resonance frequency, quality factor, mutual inductance, and maximum efficiency of the states were calculated separately. The variation of efficiency and equivalent impedance according to frequency for coupling factors 0.1 and 0.5 is shown in Fig. 2.

In WPT systems with SS topology, equivalent impedance is minimum and efficiency is maximum at resonance frequencies as seen in Fig. 2. In Fig. 2a, it is seen that (9) is provided for $k = 0.1$ and a single resonance frequency situation occurs. In Fig. 2b, it is seen that equation (10) is provided for $k = 0.5$ and a three resonance frequency situation occurs. In the case of frequency bifurcation, the lowest resonant frequency is preferred to reduce the skin effect and proximity effect on AC resistance. At the 10 kHz WPT design, the lowest resonance frequency is 8400 Hz and the equivalent impedance is 5 Ω. At the 20 kHz WPT design, the lowest resonance frequency is 16 700 Hz and the equivalent impedance is 4.94 Ω. At the resonant frequency, the equivalent impedance is minimum and efficiency is maximum. However, the equivalent impedance at the second resonance frequency is higher than the first resonance and third resonance frequency. In the case of (10), the equivalent impedance value of the second resonant frequency gets larger as the air gap decreases, and accordingly the power drawn from the input decreases. Therefore, it is not preferred to work at the second resonance frequency in WPT systems with SS topology. The circuit is set up in MATLAB/Simulink as in Fig. 3.

Output power (P_2) is fixed at 3.3 kW by adjusting the input voltage (V_1) for $k = 0.1$ and $k = 0.5$. The MATLAB/Simulink results for 10 kHz and 20 kHz are given in Table I. The top and side view of spiral inductance is shown in Fig. 4.

The self-inductance of the spiral coil was calculated using (13) and (14):

$$L = \frac{N^2 A^2}{30A - 11D_i} \tag{13}$$

$$A = \frac{D_i + N\left(W + S\right)}{2} \tag{14}$$

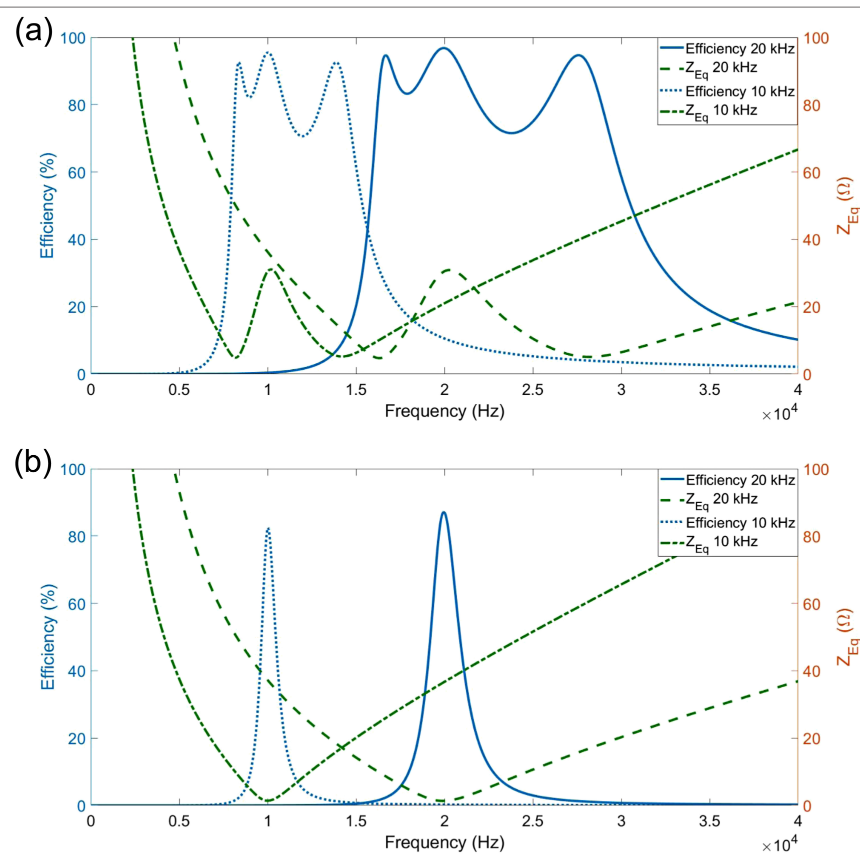

Fig. 2. Efficiency–frequency and equivalent impedance–frequency graph for 10 kHz and 20 kHz design (a) $k = 0.1$ and (b) $k = 0.5$.

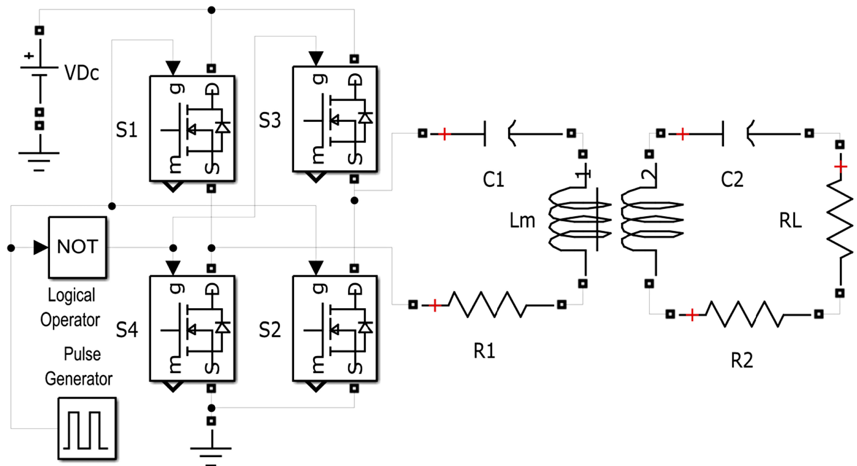

Fig. 3. Wireless power transfer circuit in MATLAB/Simulink.

TABLE I. MATLAB/SIMULINK RESULTS FOR 10 KHZ AND 20 KHZ

10 kHz				**20 kHz**			
***k* = 0.1**		***k* = 0.5**		***k* = 0.1**		***k* = 0.5**	
L_m = 39.7 µH	f_r = 10350 Hz	L_m = 199 µH	f_r = 8400 Hz	L_m = 19.89 µH	f_r = 20035 Hz	L_m = 99.5 µH	f_r = 16700 Hz
Z_{Eq} = 2 Ω	η = 81%	Z_{Eq} = 5 Ω	η = 89.19 %	Z_{Eq} = 1.43 Ω	η = 86 %	Z_{Eq} = 4.94 Ω	η = 94.64%
V_1 = 119 V	V_2 = 181 V	V_1 = 168 V	V_2 = 181 V	V_1 = 96 V	V_2 = 128.7 V	V_1 = 113.1 V	V_2 = 132.5 V
I_1 = 76.03 A	I_2 = 36.32 A	I_1 = 35.5 A	I_2 = 36 A	I_1 = 53.19 A	I_2 = 25.73 A	I_1 = 25.55 A	I_2 = 26.49 A
P_1 = 4100 W	P_2 = 3300 W	P_1 = 3700 W	P_2 = 3300 W	P_1 = 3840 W	P_2 = 3320 W	P_1 = 3508 W	P_2 = 3320 W
V_{C1} = 1850 V	V_{C2} = 860 V	V_{C1} = 1050 V	V_{C2} = 1050 V	V_{C1} = 1322.3 V	V_{C2} = 642.1 V	V_{C1} = 767.2 V	V_{C2} = 760.8 V

f_r is the resonant frequency, V_2 is the output voltage, P_1 is the input power, and η is the efficiency. V_{C1} and V_{C2} are the voltages of the resonant capacitors in the circuit at the transmitter and receiver, respectively.

N is the number of turns, D_i is the inner diameter of the coil, D_o is the outer diameter of the coil, S is the spacing between the turns, and W is the diameter of the cable. Coil parameters for 10 kHz and 20 kHz designs are given in Table II.

IV. WIRELESS POWER TRANSFER SIMULATIONS

In this study, ANSYS software, a FEM-based simulation program, was used to design the coils and examine the magnetic field scattering and electrical field distribution.

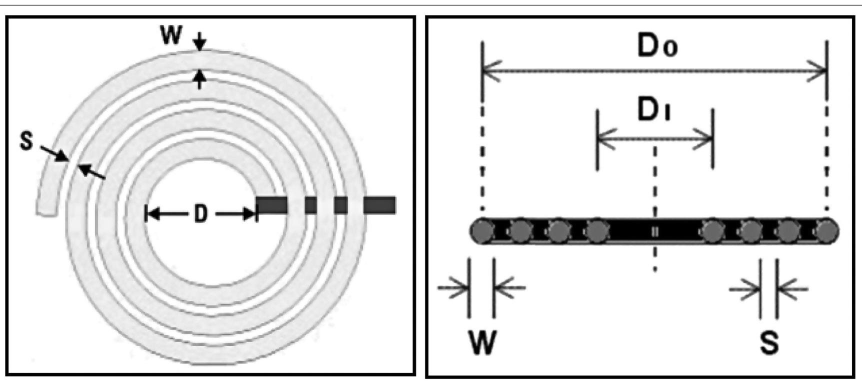

Fig. 4. Top and side view of spiral inductance.

TABLE II. COIL DESIGN PARAMETERS

Frequency	**10 kHz**	**20 kHz**
Coil outer diameter	50 cm	50 cm
Coil inner diameter	367 mm	409 mm
Number of turns	23	15
Wire diameter	1.8 mm	1.8 mm
Spacing between turns	1 mm	1 mm
Wire length	31.171 m	21.25 m
Inductance	398.107 μH	198.78 μH
Wire resistance	0.206 Ω	0.14 Ω

A. Coil Design

The transmitter and receiver coils are designed separately for the 10 kHz and 20 kHz systems. The outer diameters of the coils designed for 10 kHz and 20 kHz are the same and 50 cm. The inner diameters of the coils designed for 10 kHz and 20 kHz are 36.7 and 40.9, respectively. The designed coils are shown in Fig. 5(a) for 10 kHz and Fig. 5(b) for 20 kHz.

The variation of the self and mutual inductance value depending on the air gap of the WPT systems with 10 kHz and 20 kHz operating frequencies is shown in Figure 6.

Using (8), it was found that $L_{mcritical10} = 77.07$ μH for 10 kHz and $L_{mcritical20} = 39.79$ μH for 20 kHz. Fig. 6 shows that the critical air gap is 15 cm for 10 kHz and 17 cm for 20 kHz. The variation of the coupling coefficient according to the air gap of the WPT system is shown in Fig. 7.

In the 10 kHz WPT design, the air gaps for $k = 0.1$ and $k = 0.5$ were found to be 23.5 cm and 5.1 cm, respectively. In the 20 kHz WPT design, the air gaps for $k = 0.1$ and $k = 0.5$ were found to be 27 cm and 6.45 cm, respectively. At the same air gap values, it can be seen in Fig. 7 that the 20 kHz frequency design has a higher coupling coefficient than the 10 kHz design.

B. Co-Simulation

The equivalent circuit of the WPT system is built on the ANSYS Simplorer interface. Coils are designed in Maxwell 3D interface. The analysis of the WPT system was made by co-simulation of these two programs. The efficiency of the WPT systems, input power, and output power was observed. The co-simulation circuit of the WPT system installed in ANSYS Simplorer is shown in Fig. 8.

The input and output powers of the WPT system at 15 cm air gap for 10 kHz and 20 kHz designs are shown in Fig. 9.

As a result of co-simulation of the WPT circuit, the average power at the input and output of the system was found. The efficiency of the WPT system was 88.79% for 10 kHz and 92.74% for 20 kHz at 15 cm air gap. The variation of efficiency with frequency for coupling

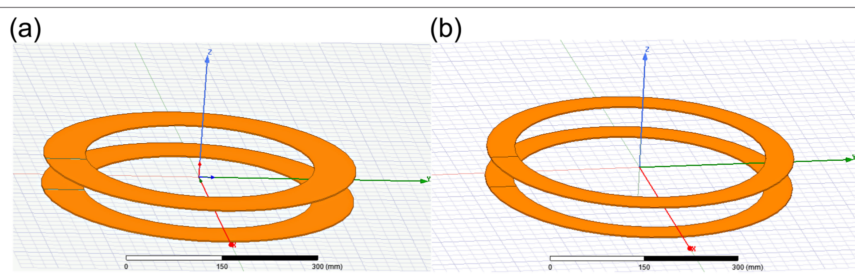

Fig. 5. Coil designs (a) 10 kHz and (b) 20 kHz.

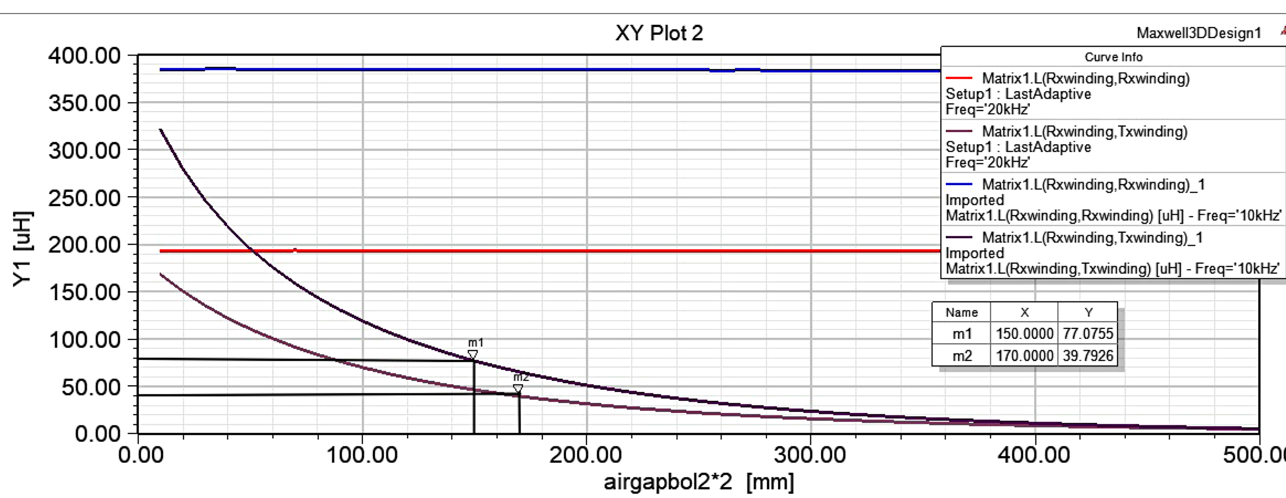

Fig. 6. Self and mutual inductance according to air gap for 10 kHz and 20 kHz wireless power transfer system.

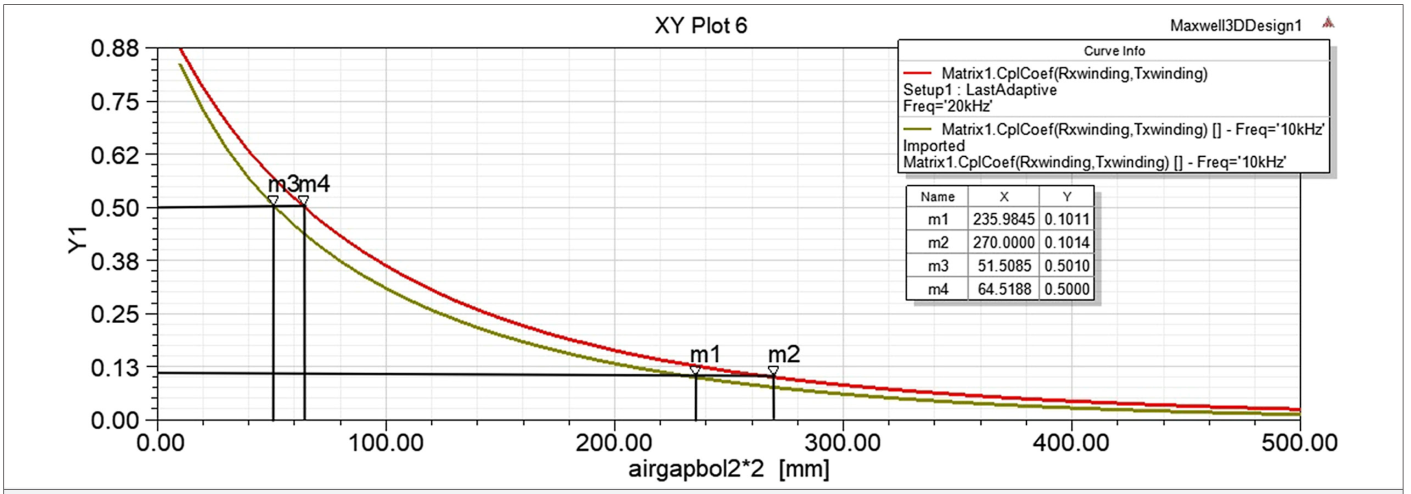

Fig. 7. Coupling coefficient according to air gap of wireless power transfer systems for 10 kHz and 20 kHz.

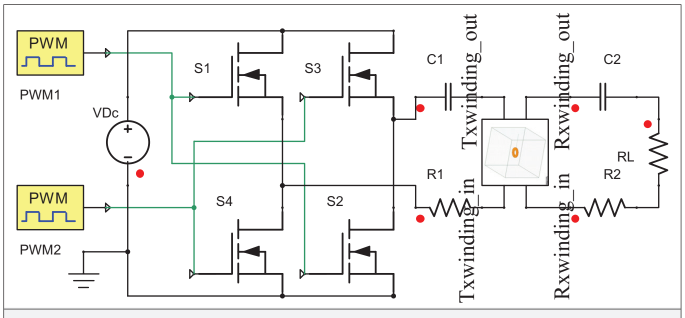

Fig. 8. The co-simulation circuit of the wireless power transfer system.

factors 0.1 and 0.5 is given in Fig. 10 by using Simplorer's AC analysis interface.

It is seen from Fig. 2 and Fig. 10 that the efficiency–frequency results obtained from the MATLAB program using the analytical circuit equations and the ANSYS Simplorer program using the FEM method are compatible with each other.

V. HUMAN HEALTH EFFECTS

Like all electronic devices, WPT systems generate electric and magnetic fields around them. In inductive coupling and magnetic resonance coupling theory-based WPT systems, the electric and magnetic field values between the receiver and the transmitter coil are high. When one moves away from the receiver and transmitter coil, the electric and magnetic field values decrease. Electrical field, magnetic field, and magnetic flux density reference values need to be known in order to determine which areas or distances in the WPT system are harmless for human health. Electric and magnetic field exposure standards of ICNIRP [16] and IEEE [17] were taken as a reference to determine the safe operating zones of the WPT system. Safe working area limits according to ICNIRP and IEEE standards for 10 kHz and 20 kHz are given in Table III [16,17].

The magnetic flux density and the electric field generated by the transmitter and receiver coils for the 10 kHz and 20 kHz designs are shown in Fig. 11.

For 10 kHz and 20 kHz, WPT designs at 15 cm air gap, the magnetic flux density and magnetic field change from the center of the

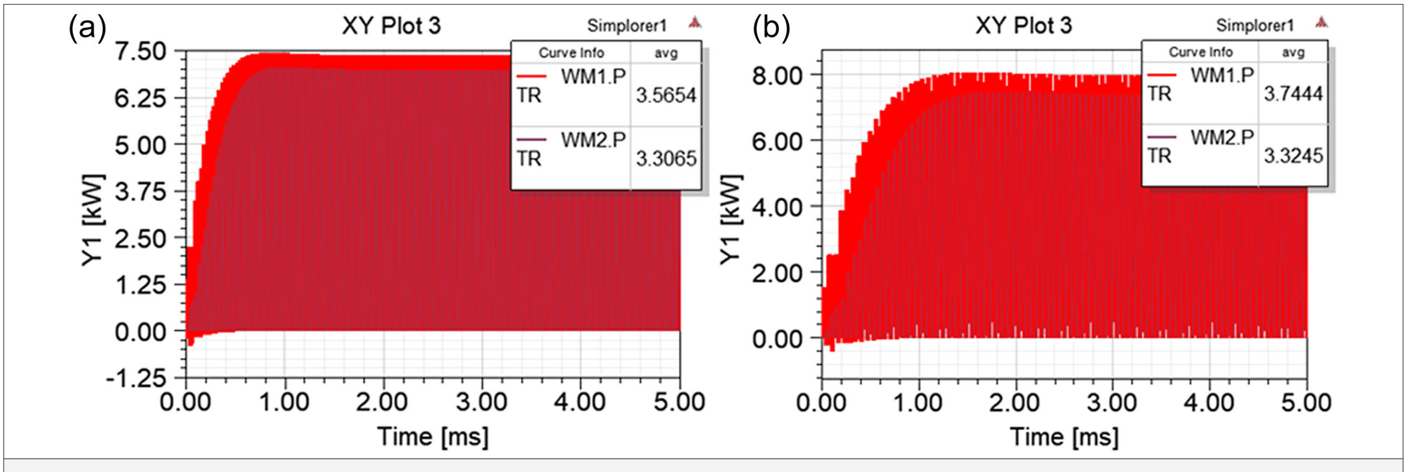

Fig. 9. Input and output power for (a) 10 kHz and (b) 20 kHz.

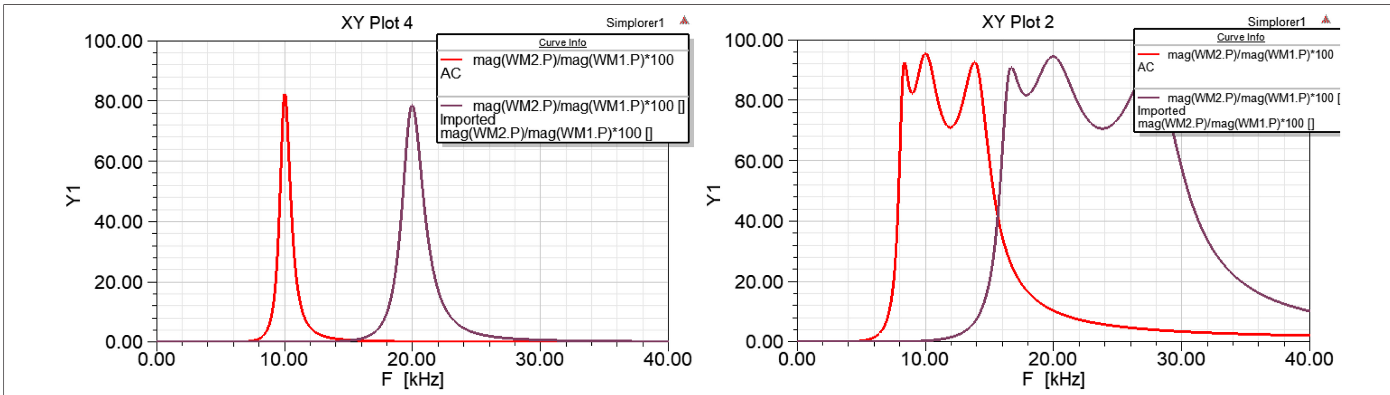

Fig. 10. Efficiency–frequency graph for (a) $k = 0.1$ and (b) $k = 0.5$.

TABLE III. SAFE AREA BOUNDARIES ACCORDING TO ICNIRP AND IEEE STANDARDS [16,17]

Standards	**Electric Field**		**Magnetic Field**		**Magnetic Flux Density**	
IEEE	Persons in unrestricted environments	Persons in restricted environments	Persons in unrestricted environments	Persons in restricted environments	Persons in unrestricted environments	Persons in unrestricted environments
IEEE (head and torso)	1842 V/m	614 V/m	163 A/m	490 A/m	205 μT	615 μT
IEEE (limbs)	1842 V/m	614 V/m	900 A/m	900 A/m	1130 μT	1130 μT
ICNIRP	Occupational exposure	Public exposure	Occupational exposure	Public exposure	Occupational exposure	Public exposure
	170 V/m	83 V/m	80 A/m	21 A/m	100 μT	27 μT

coil to the outside of the coil (in the horizontal axis) are shown in Fig. 12.

Boundaries of safe areas suitable for public and occupational exposure have been determined in Fig. 12. Safe area limits for public exposure start after 59.9 cm and 47.6 cm from the coil for the 10 kHz and 20 kHz designs, respectively. Safe area limits for occupational exposure start after 28.7 cm and 20 cm from the coil for the 10 kHz and 20 kHz designs, respectively. A female body, a male body, and a male arm were used to examine the effect of the WPT system on

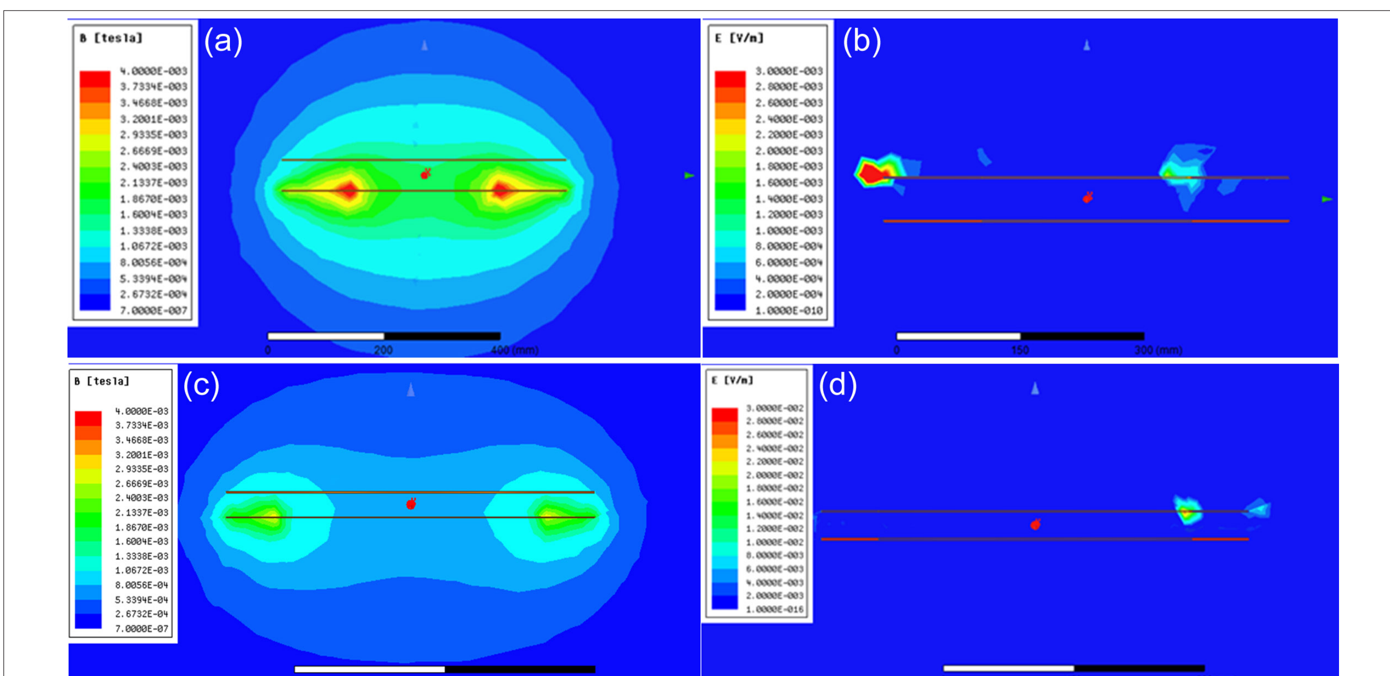

Fig. 11. (a) 10 kHz magnetic flux density, (b) 10 kHz electric field, (c) 20 kHz magnetic flux density and (d) 20 kHz electric field graph.

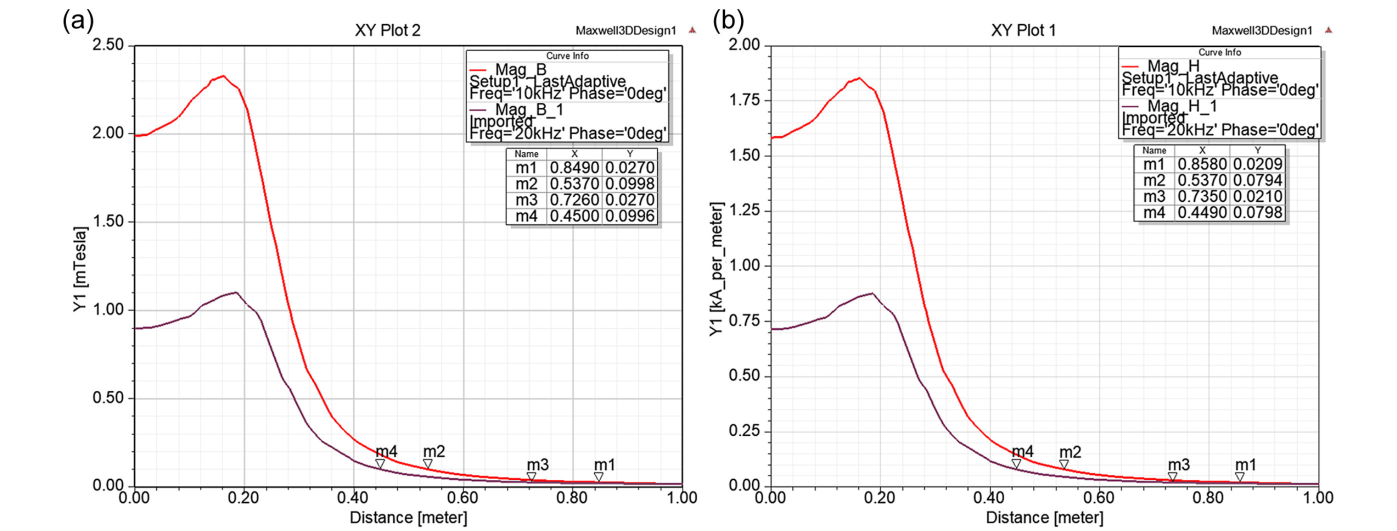

Fig. 12. (a) Magnetic flux density and (b) magnetic field from the coil center to the outside of the coil (on the horizontal axis).

human limbs. In the simulation made on the HFSS interface, the exposed electric field and magnetic field were examined. The female body was placed 25 cm away from the WPT system, the male body was placed right next to the WPT system, and the male arm was placed between the receiver and transmitter coil. For 10 kHz and 20 kHz WPT systems, the magnetic field and electric field to which the human limbs are exposed are given in Fig. 13.

In Fig. 13, it is seen that the magnetic field in the male arm placed between the receiver and the transmitter was above the ICNIRP and IEEE standards. In the male body, present right next to the WPT system, the magnetic field exposure of the right leg was above ICNIRP and IEEE standards. However, the magnetic field exposure of the left leg was below these standards. The female body, which was 25 cm away from the WPT system, was in a safe area according to ICNIRP and IEEE standards. It is seen in Fig. 12 and Fig. 13 that the magnetic field emitted by the 20 kHz design is less than the 10 kHz design. In Fig. 12 and Fig. 13, the magnetic field emitted by the 20 kHz design is less than the 10 kHz design because 20 kHz design has less inductance and less number of turns than 10 kHz design.

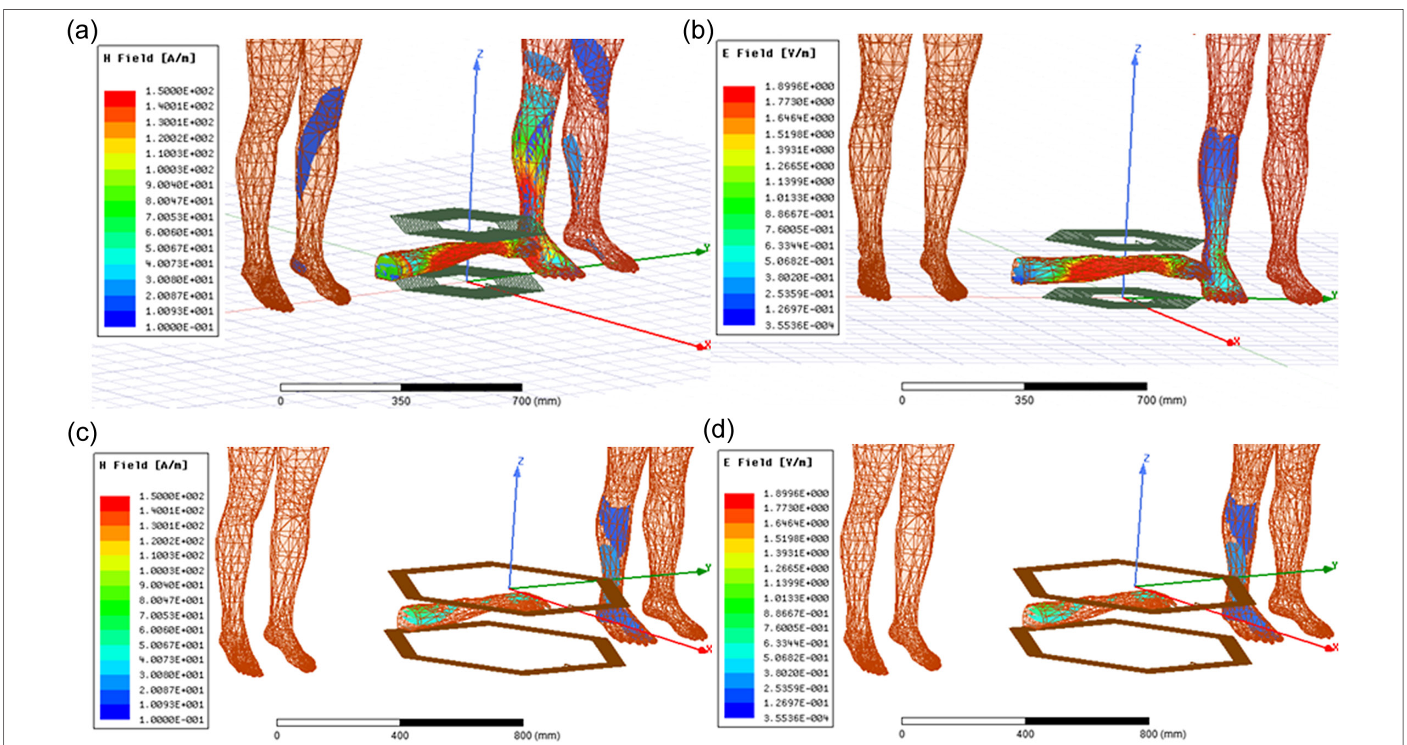

Fig. 13. Exposure graph of limbs (a) 10 kHz magnetic field, (b) 10 kHz electric field, (c) 20 kHz magnetic field, and (d) 20 kHz electric field.

VI. RESULT AND DISCUSSION

In WPT systems, there is no physical connection between the receiver and transmitter. Wireless power transfer systems eliminate cable pollution and problems. In this study, two separate WPT systems with an operating frequency of 10 kHz and 20 kHz were designed and compared with each other. The WPT circuit with SS topology was built on MATLAB/Simulink program. Coils were designed using the FEM method with the help of ANSYS® Maxwell 3D program. The change of self-inductance, mutual inductance, and coupling coefficient of the receiver and transmitter coils according to the air gap was observed. In WPT systems, the connection factor decreases as the air gap between the receiver and transmitter increases. In two designs with the same dimensions, it was observed that the connection factor values of the 20 kHz design at different air gaps were higher than the 10 kHz design. It was observed that the efficiency remained constant until the critical air gap with the decrease of the coupling coefficient, and after passing the critical air gap, the efficiency decreased due to decreasing coupling coefficient. The critical air gap for the 20 kHz and 10 kHz designs was found to be 17 cm and 15 cm, respectively. In the 15 cm air gap, the 10 kHz and 20 kHz designs transferred 3.3 kW of power to output with 88.79% and 92.74% efficiency, respectively. It has also been observed that the designs can transfer energy with higher efficiency in higher air gaps as the natural resonance frequencies increase.

In which regions the magnetic field emitted by the coils is safe and unsafe for human health has been determined according to IEEE and ICNIRP standards. In this study, it has been observed that scattering can pose a danger to human health when one is between or very close to the receiver and transmitter coil. When one moves away from the coils as much as approximately the coil diameter, a safe area for public exposure is reached in 20 kHz systems. On the other hand, in 10 kHz systems, it is necessary to move further away from the boundaries of the 20 kHz system for a safe area. In this case, it is shown that WPT systems need living and object detection systems to shut down the system when a living being or an object is between or near the receiver and transmitter. In addition, it has been observed that the magnetic field created by the 20 kHz design is less than the 10 kHz design. High-frequency designs have lower inductance values, lower number of turns, and correspondingly lower magnetic flux density.

Peer-review: Externally peer-reviewed.

Author Contributions: Concept – A.A.; Design – A.A., T.H.D., G.A.; Supervision – A.A.; Materials – A.A., T.H.D., G.A.; Data Collection and/or Processing – A.A., T.H.D.; Analysis and/or Interpretation – A.A., T.H.D.; Literature Review – A.A.; Writing Manuscript– A.A., T.H.D.; Critical Review – A.A.

Declaration of Interests: The authors declare that they have no competing interest.

Funding: The author declared that this study has received no financial support.

REFERENCES

1. A., Pashaei, E., M. Aydin, E. Polat, Yildiriz, and M. T. Aydemir, "Elektrikli Araçlar için Temassız Güç Aktarım Sistemleri," *EMO Bilimsel Dergi*, vol. 6, no. 11, pp. 1–11, 2016.
2. E., Aydin, and M. T. Aydemir, "A 1-kW wireless power transfer system for electric vehicle charging with hexagonal flat spiral coil," *Turk J. Elec Eng & Comp Sci*, vol. 29, no. 5, pp. 2346–2361, 2021. [CrossRef]
3. Z., Doğan, M., Özsoy, and İ. İskender, "*Manyetik Rezonansa Dayalı Kablosuz Enerji Transferi İçin Yeni Bir Nüve Geometrisi*", *Gazi Üniversitesi Fen Bilimleri Dergisi Part C: Tasarım ve Teknoloji*, Vol. 7, no. 4, 2019, pp. 1012–1024.
4. S., Çetin, Y. E., Demirci, O., and Buyukgumus, "Performance evaluation of a wireless charging converter for active implantable medical device," *Mugla J. Sci. Technol. (MJST)*, vol. 6, no.:2, pp. 11–17, 2020.
5. N., Tesla, *Apparatus for Transmission of Electrical Energy*, U.S. Patent No. 649, Vol. 621, 1900.
6. W. C., Brown, "Experiments involving a microwave beam to power and position a helicopter," *IEEE Trans. Aerosp. Electron. Syst.*, vol. 5, no. 1, pp. 692–702, 1969. [CrossRef]
7. G. A., Covic, and J. T. Boys, "Modern trends in inductive power transfer for transportation applications," *IEEE J. Emerg. Sel. Top. Power Electron.*, vol. 1, no. 1, pp. 28–41, 2013. [CrossRef]
8. S. A., Sis, "A circuit model-based analysis of magnetically coupled resonant loops in wireless power transfer systems," *ELECTRICA*, vol. 18, no. 2, pp. 159–166, 2018. [CrossRef]
9. A., Karalis, J. D., Joannopoulos, and M. Soljacic, "Efficient wireless nonradiative mid-range energy transfer," *Sci. Direct*, vol. 323, no. 1, pp. 34–48, 2008.
10. T. F., Skaik, and B. O., AlWadiya, "Design of wireless power transfer system with triplet coil configuration based on magnetic resonance," *ELECTRICA*, vol. 17, no. 1, pp. 3169–3174, 2017.
11. T. Imura, and Y. Hori, "Maximizing air gap and efficiency of magnetic resonant coupling for wireless power transfer using equivalent circuit and Neumann formula," *IEEE Trans. Ind. Electron.*, vol. 58, no. 10, pp. 4746–4752, 2011. [CrossRef]
12. L. H. Liang, Z. Z. Liu, Y. J. Hou, H. Zeng, Z. K. Yue, and S. Cui, "Study on frequency characteristics of wireless power transmission system based on magnetic coupling resonance," *IOP Conf. Ser.: Earth Environ. Sci.*, vol. 93, no. 1, p. 012063, 2017. [CrossRef]
13. F. Issı, and O. Kaplan, "Manyetik Rezonans Kuplajlı Kablosuz Enerji Transfer Sistemi için Empedans Analizi ve Değişken Kapasite Dizisi Uygulaması," *Gazi Üniversitesi Fen Bilimleri Dergisi Part C: Tasarım ve Teknoloji*, Vol. 8, no. 4, 2020, pp. 1005–1020.
14. S. A., Sis, and H. Akça, "Maximizing the efficiency of wireless power transfer systems with an optimal duty cycle operation," *AEU Int. J. Electron. Commun.*, vol. 116, p. 153081, 2020. [CrossRef]
15. A. Agcal, N. Bekiroglu, and S. Ozcira, "Comparison of magnetic resonant coupling wireless power transfer systems within aligned and unaligned positions and determining their limits," *J. Magn.*, vol. 21, no. 4, pp. 652–659, 2016. [CrossRef]
16. International Commission on Non-Ionizing Radiation Protection (ICNIRP), "Guidelines for limiting exposure to time-varying electric and magnetic fields for low frequencies (1 Hz–100 kHz)," *Health Phys.*, vol. 99, no. 6, pp. 818–836, 2010. [CrossRef]
17. IEEE, "*Standard for safety levels with respect to human exposure to electric, magnetic, and electromagnetic fields (0 Hz to 100 kHz)*," Std, Vol. C95, no. 1™-2019, 2019.

Ali AĞÇAL received the B.Sc., M.Sc. and PhD. degrees from the Department of Electrical Engineering, Yildiz Technical University, Istanbul in 2011, 2014 and 2017 respectively. From 2012 to 2018, He was a Research Assistant at Department of Electrical Engineering, Yildiz Technical University. In 2019, He worked as a Lecturer at Department of Electrical and Energy, Mugla Sitki Kocman University. He is presently working as a Assistant Professor at Department of Electrical and Electronics Engineering, Suleyman Demirel University. His research interests are wireless power transfer, power electronics, and electrical machines.

Tuğba Halime DOĞAN received the B.S. degree in electronics and communication engineering from Suleyman Demirel University, Isparta, Turkey. She is currently a M.Sc. student in electrical and electronics engineering at Suleyman Demirel University, Isparta, Turkey. She is presently working as a Project Engineer at Isparta Enerji San.ve Tic. Ltd. Sti. Her main resarches interest are wireless power transfer, power electronics.

Galip AKSU received the B. S. Degree in electronics and communication engineering from Suleyman Demirel University. He is presently working as a Maintenance Engineer at Anadolu Isuzu Automotive Industry & Trading A.Ş. His research areas are industrial electronics, power electronics and wireless power transfer.